ORIGINAL ARTICLE

WILEY

Somatic *GNA11/GNAQ* variants in a cohort of Chinese children with phakomatosis pigmentovascularis

Bin Zhang[1,2] | Rui He[1] | Riga Wu[1,3] | Zhou Yang[1] | Man Hu[4] | Nan Zhang[5] | Wu Guo[2] | Zigang Xu[1] | Lin Ma[1]

[1]Department of Dermatology, Beijing Children's Hospital, Capital Medical University, National Center for Children's Health, Beijing, China
[2]Department of Dermatology, Zhengzhou University, Affiliated Children's Hospital, Henan Children's Hospital, Zhengzhou Children's Hospital, Zhengzhou, China
[3]Department of Dermatology, Affiliated Hospital of Inner Mongolia Medical University, Hohhot, China
[4]Department of Ophthalmology, Beijing Children's Hospital, Capital Medical University, National Center for Children's Health, Beijing, China
[5]Department of Pathology, Beijing Children's Hospital, Capital Medical University, National Center for Children's Health, Beijing, China

Correspondence
Lin Ma, and Zigang Xu, Department of Dermatology, Beijing Children's Hospital, Capital Medical University, National Center for Children's Health, Beijing, China.
Email: bch_maleen@aliyun.com; zigangxupek@163.com

ABSTRACT

Importance: Postzygotic mutations in the *GNAQ/GNA11* genes, which encode the G-protein nucleotide binding protein alpha subunits, have been identified in patients with phakomatosis pigmentovascularis (PPV). However, little is known about the Chinese population.

Objective: To identify pathogenic mutations in pediatric patients with PPV within the Chinese population.

Methods: We performed whole-exome sequencing (WES) using skin lesion tissues from pediatric patients diagnosed with PPV. Additionally, ultradeep-targeted sequencing was conducted to validate the somatic mutations. A genotype-phenotype correlation was analyzed by integrating data from previous reports with the findings of the present study.

Results: Thirteen patients were enrolled, all diagnosed with the cesioflammea type of PPV, except for one patient with an unclassifiable type. We identified somatic *GNA11* c.547C>T (p.R183C) variant in seven patients and *GNAQ* c.548G>A (p.R183Q) in four patients, with low allelic fractions ranging from 2.1% to 8.6% through ultradeep sequencing. Besides, a *GNAQ* c.548G>A (p.R183Q) variant was detected through targeted sequencing in one of two patients who did not exhibit detectable variants via WES. The genotype-phenotype correlation analysis, involving 15 patients with a *GNA11* variant and 10 with a *GNAQ* variant, revealed that facial capillary malformation (87% *vs.* 50%, $P = 0.075$) and ocular melanocytosis (80% *vs.* 40%, $P = 0.087$) appeared to be more frequent in patients with *GNA11* mutation compared to those with *GNAQ* mutations. All four patients diagnosed with cesiomarmorata type or overlapping cesioflammea and cesiomarmorata type PPV carried the *GNA11* variant.

Interpretation: Our study demonstrated that the majority of PPV patients in the Chinese population carried a postzygotic variant of *GNAQ/GNA11*, thus further confirming the pathogenic role of *GNAQ/GNA11* mosaicism in the development of PPV cesioflammea type.

INTRODUCTION

Phakomatosis pigmentovascularis (PPV) describes a rare group of vascular and pigmentary birthmarks characterized by the co-occurrence of congenital capillary malformations (CMs) and pigmentary changes.[1] The estimated incidence of PPV is 5.8 per 100 000 pediatric patients and 0.634 per 100 000 dermatologic patients.[2] Cutis marmorata telangiectatica congenita, although extremely rare, has also been reported in several cases.[3–5] Pigmentary birthmarks encompass ectopic Mongolian spots (EMS), nevus of Ota, nevus of Ito, and café-au-lait spots.

Apart from various birthmarks, nearly half of PPV patients are accompanied by extracutaneous impairments.[6] A recent literature review study summarizing 176 PPV patients revealed a high frequency and a variety of extracutaneous manifestations, including glaucoma, hemihypertrophy, seizures, ocular melanoma, brain calcifications, ventriculomegaly, and brain atrophy.[7] These ocular and neurological abnormalities, along with overgrowth of soft tissues and limbs, overlap with the clinical features of Sturge–Weber syndrome (SWS) and Klippel–Trénaunay syndrome (KTS).[8,9] SWS is a rare CM-associated neurocutaneous disorder featured by facial CM and ocular and/or cerebral vascular malformations, leading to symptoms such as glaucoma, seizures, and cognitive delay.[10] KTS describes a rare syndrome characterized by the triad of CMs, varicose veins, and hypertrophy of soft tissue and bone.[11] SWS and KTS are the most frequently reported systemic diseases associated with PPV.

Postzygotic variants of *GNAQ*, the gene encoding the guanine nucleotide-binding protein alpha q polypeptide, are responsible for isolated CM and SWS.[12,13] The shared clinical features between SWS and PPV have led to the hypothesis that PPV may be caused by postzygotic mutation of a member of the G protein alpha subunit family. Thomas et al.[14] first identified somatic variants of *GNA11* and *GNAQ* in several patients diagnosed with PPV or extensive dermal melanocytosis. Subsequent transgenic mosaic zebrafish models expressing *GNA11*[R183C] showed dermal melanocytosis mimicking human phenotype.[14] These findings were later validated by several case reports detecting *GNAQ/GNA11* mosaic-activating variants in PPV patients.[7,15–18] The majority of reported variants hotspots were *GNA11* c.547C>T (p.R183C) and *GNAQ* c.548G>A (p.R183Q).

Till now, a limited number of PPV patients with a pathogenic *GNAQ/GNA11* variant has been described, and only one case, who had a *GNA11* variant and a second hit in *KRAS*, was reported in the Chinese population.[17] Here, we present the clinical characteristics and genetic findings in a series of pediatric patients with PPV in the Chinese population. We identified mosaic *GNAQ/GNA11* variants in 12 out of 13 patients, further confirming the pathogenic role of postzygotic *GNAQ/GNA11* variants in the development of PPV.

METHODS

Ethics approval

This study was conducted in accordance with the Declaration of Helsinki and approved by the Ethics Committee of Beijing Children's Hospital (2020-k-245). Since all participants were children, written informed consent was obtained from their parents.

Participants

Consecutive pediatric patients with PPV who were referred to the Department of Dermatology, Beijing Children's Hospital, Capital Medical University, Beijing, China were recruited from January 2019 to December 2022. The diagnoses of CM, pigmentary nevus, and extracutaneous systemic disease were performed by a dermatologist experienced in vascular anomalies. PPV subtype was classified as type I to V according to the traditional classification,[4,19] and as cesioflammea, spilorosea, cesiomarmorata, and unclassifiable type according to the classification proposed by Happle.[20] The mosaicism pattern, according to the distribution of vascular and pigmentary lesions, was classified as Blaschko lines, checkboard, phylloid, patchy pattern without midline separation and lateralization.[21] Skin biopsies, from either vascular lesion or pigmentary lesion or both when possible, and peripheral blood samples were collected from all participants.

Detection of somatic variants

Genomic DNA was extracted from fresh skin lesion samples or peripheral blood samples. For each patient, a least one tissue sample was selected for whole-exome sequencing (WES) at a mean sequencing depth of 500×. All exons were captured by using GenCap Human Exome Kit (MyGenostics Co.Ltd.) according to the

manufacturer's instruction and then were massively sequenced on the Illumina NexSeq 500 platform. After quality control, all reads were mapped to the human reference genome (hg19) using Burrows–Wheeler Aligner v0.7.10 (http://bio-bwa.sourceforge.net/). Subsequent duplication removal, insertion/deletion (indel) realignment, and base quality score recalibration were performed using Genome Analysis Toolkit (GATK) v4.0.8.1 (http://www.broadinstitute.org/gatk/). Finally, single nucleotide variants and indels were detected using GATK HaplotyperCaller and annotated by the latest version of ANNOVOR (http://www.openbioinformatics.org/annovar/). A somatic variant of *GNAQ/GNA11* should be covered by at least 5 identical variant alleles with a variant allele frequency (VAF) > 1%. VAF is defined as the number of variant reads divided by the total number of mapping reads.

Validation of somatic variants

For somatic variants identified through WES, we first viewed the mapping alignment through Integrative Genomics Viewer (IGV, http://software.broadinstitute.org/software/igv/igvtools) to exclude misalignment. Secondly, the variants were validated by ultradeep targeted sequencing in vascular and/or pigmentary lesion samples. Briefly, the variants were amplified by polymerase chain reaction using primers as follows: forward-TGCTTCAGACACTGCCGTAG and reverse-ACCGGAAGATGATGTTCTCCA for *GNA11* c.547C>T (p.R183C) variant, and forward-GAAGCCTACACATGATTCCAGT and reverse-GCTTTGGTGTGATGGTGTCA for *GNAQ* c.548G>A (p.R183Q) variant. The sequence library was constructed and sequenced on a next-generation sequencing platform, and variants were detected using the aforementioned methods in WES. The verified variant with a VAF < 1% was considered false negative as it was not possible to distinguish this from background noise. Finally, for samples without detectable *GNA11* or *GNAQ* variants through WES, ultradeep sequencing of *GNA11* c.547C>T (p.R183C) and *GNAQ* c.548G>A (p.R183Q) hotspots were both performed. Sanger sequencing of *GNAQ/GNA11* variants in peripheral blood DNA was performed to exclude germline origin.

Statistical analysis

The Fisher's exact test was used to compare categorical variables. $P < 0.05$ was considered statistically significant.

RESULTS

Clinical characteristics of PPV patients

A total of 13 pediatric patients with PPV, including six males and seven females, were enrolled. The ages ranged from 3 months to 13 years. The clinical characteristics of all patients are summarized in Table 1. Regarding vascular lesions, all patients exhibited CM, and nine presented nevus anemicus (Figure 1A–C). CM was distributed across the entire body, with nine patients displaying facial CM. As to pigmentary lesions, 11 patients had only EMS, one had only café au lait spot, and one had both EMS and café au lait spot. Additionally, nine patients presented scleral melanocytosis (Figure 1D–H). All patients exhibited a checkboard type of mosaicism pattern, except for one displaying a lateralization pattern. According to Happle's classification, 12 patients were classified as cesioflammea type, while one was classified as an unclassifiable type.

In addition to the typical vascular and pigmentary birthmarks, seven patients presented with hypertrophy of limbs or soft tissues. Among them, six patients (Patients 1, 2, 4, 6, 8, and 11) had an overgrowth of either upper or lower limbs (Figure 2A–C). Magnetic resonance imaging (MRI) of the affected limbs showed a significantly thickened fat layer and multiple reticular and strip-like high-signal shadows in the fat layer, muscle, and bone (Figure 2D). Thus, they were diagnosed with concurrent KTS. Patient 9 exhibited right facial hypertrophy with a thicker fat layer and increased shadows of small vessels compared to the contralateral side, as indicated by MRI (Figure 2E, F). He was subsequently diagnosed with diffuse CM with overgrowth. Patient 6, in addition to hypertrophic limbs, presented with glaucoma, seizures, and cognitive delay. Cerebral MRI revealed tortuous strip calcification in the bilateral temporal and occipital lobes, distributed along the brain gyri (Figure 2G, H). Therefore, a diagnosis of PPV with concomitant KTS and SWS was made for this patient.

Somatic variants in *GNAQ/GNA11*

A total of 15 skin biopsies, including 12 from vascular lesions and three from pigmentary lesions, were sequenced using the WES method. The hotspot variant of *GNA11* c.547C>T (p.R183C) was identified in eight tissue samples from seven patients, with a VAF ranging from 2.4% to 7.6%, while *GNAQ* c.548G>A (p.R183Q) was detected in five tissue samples from four patients, with a VAF varying between 2.1% and 8.6% (Table 2). The mapping alignments of both variants, showing low allelic fractions, suggested a somatic origin for these variants (Figure S1). These variants were further validated by ultradeep sequencing. Targeted sequencing of eight CM samples, two nevus anemicus samples, and five pigmentary lesion samples confirmed the presence of somatic variants of *GNAQ/GNA11* identical to those identified by WES (Table 2). Sanger sequencing performed on blood samples did not detect the corresponding *GNAQ/GNA11* variants, thus excluding a germline origin. Hematoxylin-eosin staining of pigmentary lesion samples

TABLE 1 Clinical manifestations of children with phakomatosis pigmentovascularis

Patient	Sex	Age	Vascular lesion		Pigmentary lesion		Extracutaneous finding	Systemic disease	Classification
			Diagnosis	Sites	Diagnosis	Sites			
1	F	8y	CM, NA	Trunk, LE, UE	EMS	HN, trunk, LE, UE	Left UE overgrowth	KTS	Cesioflammea (IIb)
2	F	6y	CM	Trunk, LE	EMS	Trunk	Left LE overgrowth	KTS	Cesioflammea (IIb)
3	M	4m	CM, NA	HN, trunk, UE	EMS	Trunk, LE, UE	None	None	Cesioflammea (IIa)
4	M	11y	CM, NA	Face, trunk, LE, UE	EMS	HN, trunk, UE	SM, left LE overgrowth	KTS	Cesioflammea (IIb)
5	F	2y	CM, NA	Face, trunk, LE, UE	EMS	Trunk	SM	None	Cesioflammea (IIa)
6	M	13y	CM, NA	Face, trunk, LE, UE	EMS	HN, trunk, LE, UE	SM, glaucoma, left LE overgrowth, seizures, and cognitive delay	SWS, KTS	Cesioflammea (IIb)
7	F	6y	CM, NA	Face, HN, trunk, LE	EMS	Eyelid, trunk	SM	None	Cesioflammea (IIa)
8	F	5y	CM	HN, trunk, LE, UE	Café au lait spot	Trunk	Right LE overgrowth	KTS	Unclassifiable (IVb)
9	M	5y	CM, NA	Face, HN, trunk, UE, LE	EMS, Café au lait spot	Trunk, LE, UE	SM, right facial overgrowth	DCMO	Cesioflammea (IIb)
10	F	3m	CM	Face, trunk, LE, UE	EMS	HN, trunk, LE, UE	SM	None	Cesioflammea (IIa)
11	M	10y	CM, NA	Face, HN, trunk, UE, LE	EMS	Trunk	SM, left LE overgrowth	KTS	Cesioflammea (IIb)
12	M	2y	CM	Face, Trunk, LE	EMS	HN, trunk, LE, UE	SM	None	Cesioflammea (IIa)
13	F	2y	CM, NA	Face, HN, trunk, UE	EMS	HN, trunk, UE	SM	None	Cesioflammea (IIa)

Abbreviations: CM, capillary malformation; DCMO, diffuse capillary malformation with overgrowth; EMS, ectopic Mongolian spot; F, female; m, month; HN, head and neck; KTS, Klippel–Trénaunay syndrome; LE, lower extremities; M, male; NA, nevus anemicus; SM, scleral melanocytosis; SWS, Sturge–Weber syndrome; UE, upper extremities; y, year.

from two patients carrying a *GNA11* and *GNAQ* somatic variant, respectively, showed the presence of nevus cells in the dermis (Figure S2).

No somatic variants of *GNAQ/GNA11* were detected in two individuals (Patients 10 and 12) via WES. Subsequently, ultradeep targeted sequencing of both *GNA11* p.R183C and *GNAQ* p.R183Q hotspots was performed (Table 2). Of patient 12, a somatic *GNAQ* c.548G>A (p.R183Q) variant was identified in the CM sample at a low allelic fraction (7.8%). However, neither *GNA11* nor *GNAQ* hotspot variants were found through ultradeep sequencing in Patient 10.

Taken together, somatic variants of *GNAQ/GNA11* were detected in 92.3% (12/13) of PPV patients in our study, with *GNA11* p.R183C identified in seven patients and *GNAQ* p.R183Q in five patients.

Genotype-phenotype correlation

We performed a genotype-phenotype correlation analysis for *GNAQ/GNA11* variants in patients with PPV by integrating data from previous reports with the findings of the present study. A literature search was conducted on PubMed for articles reporting somatic variants in PPV patients until January 31, 2023. Six studies were identified, detecting somatic *GNAQ/GNA11* variants in 13 out of 17 patients with PPV.[7,14–18] Thomas et al.[14] reported three additional patients with extensive dermal melanocytosis but without lesions, two of whom had a *GNAQ* variant. These three cases were discarded from our analysis as they
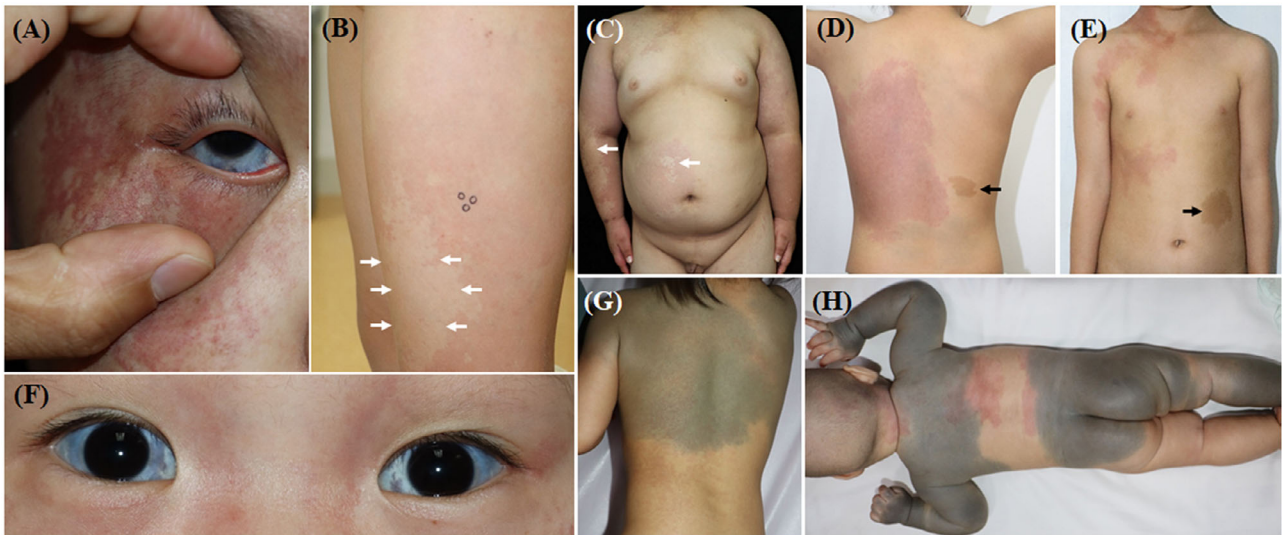
FIGURE 1 The lesions of all types of PPV showed irregular erythema in a mosaic pattern, with clear and irregular boundaries. Some patients followed by nevus anemicus (B, C white arrow). In addition to the above vascular lesions, pigmentary lesions can be shown as café-au-lait spots (D, E, black arrow), scleral melanocytosis (A, F), and ectopic Mongolian spots (G, H). These photos showed clinical manifestations corresponding to Patient 11 (A), Patient 7 (B), Patient 4 (C), Patient 2 (D), Patient 8 (E), Patient 9 (F), Patient 13 (G), and Patient 3 (H), respectively. PPV, phakomatosis pigmentovascularis.
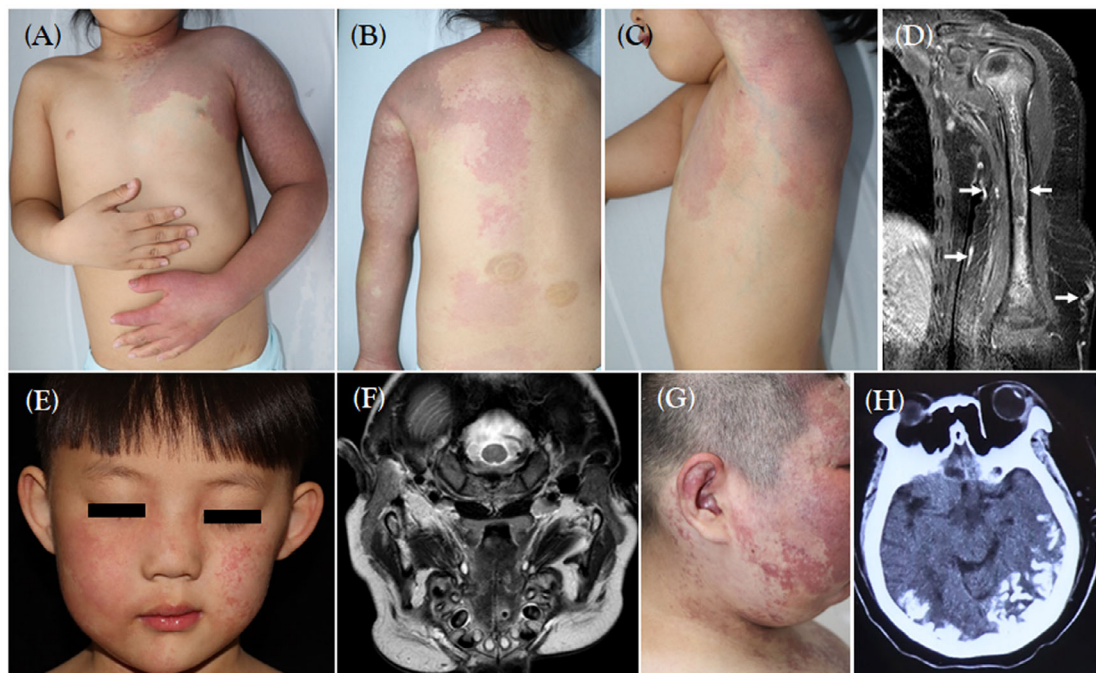

FIGURE 2 Systemic involvement of PPV. (A–D) Patient 1 with KTS, the affected limb was thickened compared with the opposite side. MRI indicated that the fat layer was significantly thickened, and there were multiple network high-signal shadows (white arrow) in the fat layer, muscle, and bone. (E, F) Patient 9 with DCMO, MRI indicated that the fat layer was locally thickened compared with the opposite side, and the empty small blood vessel shadow was increased. (G, H) Patient 6 with SWS, cranial MRI indicated tortuosity strip calcification in bilateral temporal and occipital lobes, distributed along gyri. DCMO, diffuse capillary malformation with overgrowth; KTS, Klippel–Trénaunay syndrome; MRI, magnet resonance imaging; PPV, phakomatosis pigmentovascularis; SWS, Sturge–Weber syndrome.

TABLE 2 Somatic *GNAQ/GNA11* variants in patients with phakomatosis pigmentovascularis

Patient	Variant	VAF (vascular skin lesion), *n/N* (%)		VAF (pigmentary skin lesion), *n/N* (%)	
		WES	Ultradeep sequencing	WES	Ultradeep sequencing
1	*GNAQ* c.548G>A (p.R183Q)	28/431 (6.5)	-	-	-
2	*GNAQ* c.548G>A (p.R183Q)	12/580 (2.1)	377/9554 (3.9)	-	-
3	*GNAQ* c.548G>A (p.R183Q)	25/292 (8.6)	18 701/147 860 (12.6)	7/189 (3.7)	46 882/841 415 (5.6)
4	*GNA11* c.547C>T (p.R183C)	12/343 (3.5)	12 551/216 816 (5.8)	10/424 (2.4)	8220/200 229 (4.1)
5	*GNA11* c.547C>T (p.R183C)	19/354 (5.4)	13 972/218 312 (6.4)	-	366/17 653 (2.1)
6	*GNA11* c.547C>T (p.R183C)	18/334 (5.4)	557 300/7 181 179 (7.8)	-	-
7	*GNA11* c.547C>T (p.R183C)	28/684 (4.1)	14 479/230 422 (6.3) 713/23 665 (3.0)[†]	-	-
8	*GNAQ* c.548G>A (p.R183Q)	6/177 (3.4)	9764/212 334 (4.6)	-	-
9	*GNA11* c.547C>T (p.R183C)	-	-	18/478 (3.8)	16 661/280 553 (5.9)
10	-	Not found[‡]	Not found[‡]	-	Not found[‡]
11	*GNA11* c.547C>T (p.R183C)	39/513 (7.6)	14 256/230 475 (6.2) 79 755/649 874 (12.3)[†]	-	-
12	*GNAQ* c.548G>A (p.R183Q)	Not found[‡]	73 727/950 632 (7.8)	-	-
13	*GNA11* c.547C>T (p.R183C)	32/537 (6.0)	-	-	13 382/728 172 (1.8)

[†]Ultradeep sequencing using nevus anemicus tissue samples.
[‡]No variants found in *GNA11* or *GNAQ*.
Abbreviations: VAF, variant allele frequency, indicated as count of variant reads/ total count of mapping reads; WES, whole-exome sequencing.

were not typical PPVs. Furthermore, two studies reporting *PTPN11* somatic variants in PPV spilorosea type, a subtype clinically distinguished from subtypes caused by *GNAQ/GNA11* variants, were also excluded.[22,23]

The clinical characteristics, including facial CM, ocular melanocytosis, glaucoma, neurological abnormalities, and overgrowth, of patients carrying *GNAQ/GNA11* mosaic variants in previous and present studies were extracted and tabulated (Table S1). In total, there were 15 PPV patients with a *GNA11* somatic variant and 10 with a *GNAQ* mosaic variant (Table 3). It seemed that facial CM (87% *vs.* 50%, *P* = 0.075) and ocular melanocytosis (80% *vs.* 40%, *P* = 0.087) were more frequently observed in patients carrying a *GNA11* variant compared to those harboring a *GNAQ* variant (Table 3). However, these differences were not statistically significant and were most likely driven by the inclusion of our study. In our study, seven patients having a *GNA11* variant presented with facial CM and ocular melanocytosis, whereas only one out of five patients with a *GNAQ* variant showed these characteristics. The incidences of glaucoma, neurological abnormalities, and overgrowth did not differ between the groups.

According to Happle's classification, there were 18 cases of cesioflammea type, three cases of cesiomarmorata type, 1 case of overlapping cesioflammea and cesiomarmorata type, and three cases of unclassifiable type PPV. *GNAQ* variants were more likely to be associated with

TABLE 3 Genotype-phenotype correlation of *GNAQ/GNA11* variants in patients with phakomatosis pigmentovascularis

Phenotype	*GNA11* (*n*=15), *n* (%)	*GNAQ* (*n* = 10), *n* (%)	*P*
Facial capillary malformation	13 (87)	5 (50)	0.075
Ocular melanocytosis	12 (80)	4 (40)	0.087
Glaucoma	4 (27)	2 (20)	1.000
Neurological abnormalities	4 (27)	2 (20)	1.000
Overgrowth	6 (40)	6 (60)	0.428
Subtypes			
Cesioflammea	9 (60)	9 (90)	0.102
Cesiomarmorata[†]	4 (27)	0 (0)	0.075
Unclassifiable	2 (13)	1 (10)	0.802

[†]Including overlapping cesioflammea and cesiomarmorata type.

cesioflammea type (90% *vs.* 60%, *P* = 0.102), whereas all four patients with cesiomarmorata type or overlapping cesioflammea and cesiomarmorata type carried the *GNA11* p.R183C hotspot (27% *vs* 0%, *P* = 0.075) (Table 3).

DISCUSSION

In the present study, we reported 13 pediatric patients diagnosed with PPV and identified postzygotic mosaicisms of *GNAQ/GNA11* in 92.3% (12/13) of these patients. To the

best of our knowledge, this study has the largest sample size for genetic analysis of PPV and is the first report of PPV case series with a pathogenic variant in the Chinese population.

Genetic analyses have identified postzygotic *GNAQ/GNA11* variants as the major etiology of PPV.[7,14–18] Almost all of the identified variants were *GNA11* p.R183C or *GNAQ* p.R813Q hotspots. Thomas et al.[14] found a novel *GNA11* p.R183S variant in a patient with PPV cesioflammea type and a *GNAQ* p.Q209P variant in a patient with a large dermal melanocytosis. The Q209 and R183 codons of *GNAQ/GNA11* are both located within the GTP binding pocket of the Gα subunit, an essential domain for hydrolysis GTP to GDP to inactivate downstream signaling.[24] Variants at these sites diminish the GTPase activity, resulting in the constitutive activation of the downstream MAPK pathway.[24] In our study, histopathology staining showed the presence of nevus cells in the dermis of patients carrying a *GNAQ/GNA11* variant, similar to the clearly visible melanocytes found in the dermis in *GNA11* mutant zebrafish.[14] The consistent phenotype observed in both patients and mosaic zebrafish models strongly supports the causal link between *GNAQ/GNA11* activating variants and the underlying mechanism of PPV development.

Despite the similar mechanisms of *GNA11* and *GNAQ* variants, it is interesting that isolated CM and SWS are mainly caused by *GNAQ* mosaicism,[12,13] whereas PPV is due to mosaicism of both genes. KTS is another extracutaneous systemic disorder seen in PPV patients.[25,26] Typically, KTS is caused by somatic variants in *PIK3CA*.[11,27] In our cohort, six out of 13 PPV patients had concurrent KTS. WES of CM tissue samples from these patients detected *GNAQ/GNA11* somatic variants but failed to find any pathogenic *PIK3CA* variants. The exact mechanism underlying these phenomena that the same variant causes distinct phenotypes needs further elucidation.

Somatic *GNAQ/GNA11* variants are the major cause of uveal melanoma, the most common intraocular cancer.[28,29] The variants mainly occur in codon Q209 and, to a lesser extent, affect codon R183.[29] Ocular and dermal melanocytosis, one of the major features of PPV, and uveal melanoma are both within the category of intradermal melanocytic proliferations.[30] Despite a different variant spectrum, the overlapping genetic etiology may predispose PPV patients to uveal melanoma.[31] It is estimated that one in 400 patients with oculo (dermal) melanocytosis develop uveal melanoma in their lifetime.[32] A literature review summarized that nearly 20% of PPV patients with ocular melanocytosis had ocular melanoma.[7] In the present study, nine of 13 patients presented scleral melanocytosis but none of them had uveal melanoma, which may be partially due to their young ages. Nonetheless, it is important to note that PPV patients with melanocytosis are at a high risk of developing uveal melanoma. Therefore, routine ophthalmic examination and imaging are recommended for PPV patients with ocular involvement to facilitate early diagnosis.[7]

Postzygotic mosaicisms of *GNAQ/GNA11* predominantly lead to cesioflammea, cesiomarmorata, and unclassifiable types of PPV. Thomas et al.[14] failed to detect somatic *GNAQ/GNA11* variants in a patient diagnosed with PPV spilorosea by targeted sequencing. PPV spilorosea, or type III according to the traditional classification, is characterized by the coexistence of nevus spilus and CM. Additionally, it may also be accompanied by skeletal and neurological abnormalities.[33] In a recent study including nine patients with PPV spilorosea or large nevus spilus, Polubbothu et al.[23] discovered mosaic missense variants in *PTPN11*, including p.A461T, p.T468M and p.V428L, in 8 patients at allelic fractions varying between 2% and 22%. *In vitro* experiments showed that *PTPN11* missense variants overactivated the downstream MAPK pathway and widely disrupted human endothelial cell angiogenesis.[23] Another study reported a case of PPV spilorosea with significant neurologic impairment and identified a mosaic *PTPN11* p.A461T variant.[22] Germline heterozygous variants of *PTPN11* are known causes of the autosomal dominant Leopard syndrome, a severe multisystemic disorder involving the eye, ear, cardiovascular system, male genitalia, and growth.[34,35] These two studies have expanded the phenotype spectrum of *PTPN11* variants and highlighted the possibility of PPV spilorosea patients passing on the variant to their offspring, leading to germline Leopard syndrome.[22,23] Taken together, the identification of postzygotic mosaicisms of *GNAQ/GNA11* and *PTPN11* supports the hypothesis that a single variant originating in a pluripotent progenitor cell is responsible for the development of various PPV subtypes.[14] Moreover, these findings improve our understanding of the pathogenesis of PPV, facilitate the development of targeted therapies, and help to achieve better clinical management

In conclusion, we identified postzygotic variants of *GNAQ/GNA11* in 92.3% (12/13) of pediatric patients with PPV in the Chinese population. Our study further confirms that *GNAQ/GNA11* mosaicism is the major genetic cause of the PPV cesioflammea type.

ACKNOWLEDGMENTS

CONFLICT OF INTEREST

The authors declare no conflict of interest.

REFERENCES

1. Oat M, Kawamura T, Ito N. Phakomatosis pigmentovascularis. *Jpn J Dermatol.* 1947;52:1-31.

2. Vidaurri-de la Cruz H, Tamayo-Sánchez L, Durán-McKinster C, Orozco-Covarrubias Mde L, Ruiz-Maldonado R. Phakomatosis pigmentovascularis II A and II B: clinical findings in 24 patients. *J Dermatol.* 2003;30:381-388. DOI: 10.1111/j.1346-8138.2003.tb00403.x

3. Du G, Zhang X, Zhang T. Cutis marmorata telangiectatica congenita and aberrant Mongolian spots: type V phacomatosis pigmentovascularis or phacomatosis cesiomarmorata. *JAAD Case Rep.* 2016;2:28-30. DOI: 10.1016/j.jdcr.2015.10.006

4. Torrelo A, Zambrano A, Happle R. Cutis marmorata telangiectatica congenita and extensive Mongolian spots: type 5 phacomatosis pigmentovascularis. *Br J Dermatol.* 2003;148:342-345. DOI: 10.1046/j.1365-2133.2003.05118.x

5. Torrelo A, Zambrano A, Happle R. Large aberrant Mongolian spots coexisting with cutis marmorata telangiectatica congenita (phacomatosis pigmentovascularis type V or phacomatosis cesiomarmorata). *J Eur Acad Dermatol Venereol.* 2006;20:308-310. DOI: 10.1111/j.1468-3083.2006.01395.x

6. Kim YC, Park HJ, Cinn YW. Phakomatosis pigmentovascularis type IIa with generalized vitiligo. *Br J Dermatol.* 2002;147:1028-1029. DOI: 10.1046/j.1365-2133.2002.49868.x

7. Kumar A, Zastrow DB, Kravets EJ, Beleford D, Ruzhnikov M, Grove ME, et al. Extracutaneous manifestations in phacomatosis cesioflammea and cesiomarmorata: case series and literature review. *Am J Med Genet A.* 2019;179:966-977. DOI: 10.1002/ajmg.a.61134

8. Namiki T, Takahashi M, Nojima K, Ueno M, Hanafusa T, Tokoro S, et al. Phacomatosis pigmentovascularis type IIb: a case with Klippel-Trenáunay syndrome and extensive dermal melanocytosis as nevus of Ota, nevus of Ito and ectopic Mongolian spots. *J Dermatol.* 2017;44:e32-e33. DOI: 10.1111/1346-8138.13505

9. Sen S, Bala S, Halder C, Ahar R, Gangopadhyay A. Phakomatosis pigmentovascularis presenting with Sturge-Weber syndrome and Klippel-Trenaunay syndrome. *Indian J Dermatol.* 2015;60:77-79. DOI: 10.4103/0019-5154.147801

10. Comi AM. Update on Sturge-Weber syndrome: diagnosis, treatment, quantitative measures, and controversies. *Lymphat Res Biol.* 2007;5:257-264. DOI: 10.1089/lrb.2007.1016

11. Harnarayan P, Harnanan D. The Klippel-Trénaunay syndrome in 2022: unravelling its genetic and molecular profile and its link to the limb overgrowth syndromes. *Vasc Health Risk Manag.* 2022;18:201-209. DOI: 10.2147/VHRM.S358849

12. Nakashima M, Miyajima M, Sugano H, Iimura Y, Kato M, Tsurusaki Y, et al. The somatic *GNAQ* mutation c.548G>A (p.R183Q) is consistently found in Sturge-Weber syndrome. *J Hum Genet.* 2014;59:691-693. DOI: 10.1038/jhg.2014.95

13. Shirley MD, Tang H, Gallione CJ, Baugher JD, Frelin LP, Cohen B, et al. Sturge-Weber syndrome and port-wine stains caused by somatic mutation in *GNAQ*. *N Engl J Med.* 2013;368:1971-1979. DOI: 10.1056/NEJMoa1213507

14. Thomas AC, Zeng Z, Rivière JB, O'Shaughnessy R, Al-Olabi L, St-Onge J, et al. Mosaic activating mutations in *GNA11* and *GNAQ* are associated with phakomatosis pigmentovascularis and extensive dermal melanocytosis. *J Invest Dermatol.* 2016;136:770-778. DOI: 10.1016/j.jid.2015.11.027

15. Minami Y, Okamoto T, Hirotsu Y, Amemiya K, Osada A, Tsukamoto K, et al. Phacomatosis pigmentovascularis type IIb with Klippel-Trenaunay syndrome: association with *GNAQ* mutation in vascular endothelial cells. *J Dermatol.* 2022;49:e444-e445. DOI: 10.1111/1346-8138.16538

16. Sliepka JM, McGriff SC, Rossetti LZ, Bizargity P, Streff H, Lee YS, et al. *GNA11* brain somatic pathogenic variant in an individual with phacomatosis pigmentovascularis. *Neurol Genet.* 2019;5:e366. DOI: 10.1212/NXG.0000000000000366

17. Sun Y, Su L, Rao Y, Wang Z, Wang D, Fan X, et al. Mosaic *GNA11* mutations and a second hit in *KRAS* in phacomatosis pigmentovascularis are associated with intraosseous arteriovenous malformations in the jaw. *J Eur Acad Dermatol Venereol.* 2022;36:e484-e486. DOI: 10.1111/jdv.17973

18. Thanos A, Shwayder T, Papakostas TD, Corradetti G, Capone A Jr, Sarraf D, et al. Retinal vascular abnormalities in phacomatosis pigmentovascularis. *Ophthalmol Retina.* 2019;3:1098-1104. DOI: 10.1016/j.oret.2019.07.004

19. Colin TS, Kumarasinghe Sujith PW. Phacomatosis pigmentovascularis type IIB: a case report. *J Dermatol.* 2004;31:415-418. DOI: 10.1111/j.1346-8138.2004.tb00695.x

20. Happle R. Phacomatosis pigmentovascularis revisited and reclassified. *Arch Dermatol.* 2005;141:385-388. DOI: 10.1001/archderm.141.3.385

21. Kouzak SS, Mendes MS, Costa IM. Cutaneous mosaicisms: concepts, patterns and classifications. *An Bras Dermatol.* 2013;88:507-517. DOI: 10.1590/abd1806-4841.20132015

22. Maione V, Soglia S, Miccio L, Calzavara-Pinton P, Napolitano A, Cinquina V, et al. Phacomatosis pigmentovascularis spilorosea and mutation in the *PTPN11* gene: new case with significant neurologic impairment. *J Dtsch Dermatol Ges.* 2022;20:1133-1136. DOI: 10.1111/ddg.14786

23. Polubothu S, Bender N, Muthiah S, Zecchin D, Demetriou C, Martin SB, et al. *PTPN11* mosaicism causes a spectrum of pigmentary and vascular neurocutaneous disorders and predisposes to melanoma. *J Invest Dermatol.* 2023;143:1042-1051. DOI: 10.1016/j.jid.2022.09.661e3

24. Coleman DE, Berghuis AM, Lee E, Linder ME, Gilman AG, Sprang SR. Structures of active conformations of Gi alpha 1 and the mechanism of GTP hydrolysis. *Science.* 1994;265:1405-1412. DOI: 10.1126/science.8073283

25. Finklea LB, Mohr MR, Warthan MM, Darrow DH, Williams JV. Two reports of phacomatosis pigmentovascularis type IIb, one in association with Sturge-Weber syndrome and Klippel-Trenaunay syndrome. *Pediatr Dermatol.* 2010;27:303-305. DOI: 10.1111/j.1525-1470.2010.01144.x

26. Garg A, Gupta LK, Khare AK, Kuldeep CM, Mittal A, Mehta S. Phacomatosis cesioflammea with Klippel Trenaunay syndrome: a rare association. *Indian Dermatol Online J.* 2013;4:216-218. DOI: 10.4103/2229-5178.115522

27. Keppler-Noreuil KM, Rios JJ, Parker VE, Semple RK, Lindhurst MJ, Sapp JC, et al. PIK3CA-related overgrowth spectrum (PROS): diagnostic and testing eligibility criteria, differential diagnosis, and evaluation. *Am J Med Genet A.* 2015;167A:287-295. DOI: 10.1002/ajmg.a.36836

28. Van Raamsdonk CD, Bezrookove V, Green G, Bauer J, Gaugler L, O'Brien JM, et al. Frequent somatic mutations of *GNAQ* in uveal melanoma and blue naevi. *Nature.* 2009;457:599-602. DOI: 10.1038/nature07586

29. Van Raamsdonk CD, Griewank KG, Crosby MB, Garrido MC, Vemula S, Wiesner T, et al. Mutations in *GNA11* in uveal melanoma. *N Engl J Med.* 2010;363:2191-2199. DOI: 10.1056/NEJMoa1000584

30. Zembowicz A, Mihm MC. Dermal dendritic melanocytic proliferations: an update. *Histopathology.* 2004;45:433-451. DOI: 10.1111/j.1365-2559.2004.01975.x

31. Singh AD, De Potter P, Fijal BA, Shields CL, Shields JA, Elston RC. Lifetime prevalence of uveal melanoma in white patients with oculo(dermal) melanocytosis. *Ophthalmology.* 1998;105:195-198. DOI: 10.1016/s0161-6420(98)92205-9

32. Shields CL, Kaliki S, Livesey M, Walker B, Garoon R, Bucci M, et al. Association of ocular and oculodermal melanocytosis with the rate of uveal melanoma metastasis: analysis of 7872 consecutive eyes. *JAMA Ophthalmol.* 2013;131:993-1003. DOI: 10.1001/jamaophthalmol.2013.129

33. Fink C, Happle R, Enk A, Haenssle HA. Phacomatosis spilorosea: visual diagnosis and associated pathologies of a rare entity. *J Eur Acad Dermatol Venereol.* 2016;30:e69-e70. DOI: 10.1111/jdv.13312

34. Coppin BD, Temple IK. Multiple lentigines syndrome (LEOPARD syndrome or progressive cardiomyopathic lentiginosis). *J Med Genet.* 1997;34:582-586. DOI: 10.1136/jmg.34.7.582

35. Digilio MC, Conti E, Sarkozy A, Mingarelli R, Dottorini T, Marino B, et al. Grouping of multiple-lentigines/LEOPARD and Noonan syndromes on the *PTPN11* gene. *Am J Hum Genet.* 2002;71:389-394. DOI: 10.1086/341528

SUPPORTING INFORMATION

Additional Supporting Information may be found online in the supporting information tab for this article.